Dielectric relaxation and dielectric decrement in ionic acetamide deep eutectic solvents: Spectral decomposition and comparison with experiments

Dhrubajyoti Maji and Ranjit Biswas*

Department of Chemical and Biological Sciences, S. N. Bose National Centre for Basic Sciences, Block-JD, Sector III, Salt Lake, Kolkata, West Bengal 700106, India

Abstract

Frequency dependent dielectric relaxation in the three deep eutectic solvents (DESs), (acetamide+$LiClO_4$/NO_3/Br), was investigated in the temperature range, $329 \leq T/K \leq 358$, via molecular dynamics (MD) simulations. Subsequently, decomposition of the real and the imaginary components of the simulated dielectric spectra was carried out to separate the rotational (dipole-dipole), translational (ion-ion) and ro-translational (dipole-ion) contributions. The dipolar contribution, as expected, was found to dominate all the frequency dependent dielectric spectra over the entire frequency regime, while the other two components together made tiny contributions only. The translational (ion-ion) and the cross ro-translational contributions appeared in the THz regime in contrast to the viscosity dependent dipolar relaxations that dominated the MHz-GHz frequency window. Our simulations predicted, in agreement with experiments, anion dependent decrement of the static dielectric constant ($\varepsilon_s \sim 20$ - 30) for acetamide ($\varepsilon_s \sim 66$) in these ionic DESs. Simulated dipole-correlations (Kirkwood g factor) indicated significant orientational frustrations. The frustrated orientational structure was found to be associated with the anion dependent damage of the acetamide H-bond network. Single dipole reorientation time distributions suggested slowed down acetamide rotations but did not indicate presence of any 'rotationally frozen' molecules. The dielectric decrement is, therefore, largely static in origin. This provides a new insight into the ion dependence of the dielectric behaviour of these ionic DESs. A good agreement between the simulated and the experimental timescales was also noticed.

Keywords: Deep eutectic solvents, Dielectric relaxations, Computer simulations, Dielectric decrement, Experiments

---

*For correspondence: ranjit@bose.res.in (RB)

I. INTRODUCTION

Deep eutectic solvents (DESs) constitute a unique class of liquid systems possessing immense potential as less hazardous alternatives to conventional organic solvents for a variety of applications in chemical industries.[1–4] DESs are multicomponent mixtures in molten phase of solid compounds mixed at particular compositions where the liquid phase is accessed through heating at higher temperatures, followed by normal cooling to room temperature or near room temperature. By definition, the liquid phase temperature must be significantly lower than the individual melting temperatures of the mixture components and as a result, is distinctly different from the prediction based on depression of freezing point via colligative effects.[5] Often, the term DESs is used somewhat loosely to encompass the molten phase of the multicomponent mixtures at temperatures and compositions that are away from those corresponding to the eutectic points.[6–12] Several outstanding solvent features, such as, viscosity and polarity turnabilities, relatively lesser environmental footprints, easy to prepare and handle, low vapor pressure, wider thermal and electrochemical windows, etc. have made DESs as popular solvents as reaction media not only for targeted chemical synthesis but also for engineering materials related to technological applications. Naturally therefore, DESs are finding applications in extraction of natural compounds[13], gas absorption[14], synthesis of targeted biopolymers[15] and organic compounds. [16] Recently, ionic DESs have been emerged as potential non-flammable electrolytes for lithium-ion batteries.[17,18]

Ionic deep eutectic solvents act as a bridge between ionic liquids (ILs) and electrolyte solutions. Ionic DESs are comprised of hydrogen bond donors (HBD) and ions generated from the dissociation of the added electrolytes. Substantial charge delocalization induced by the extensive interspecies (ion-amide) H-bond interactions causing frustrations in the ionic lattices provides the enthalpic support for formation of DESs.[19–22] The entropy gains for being in the liquid phase then completes the driving force behind the stable liquidous regime in DESs, although theoretical/computational investigation for the composition and temperature dependent entropy gain (both rotational and translational) are still unavailable. Different experiments, such as, time-resolved fluorescence experiments,[6,8,9,23–25] dielectric relaxation and conductivity measurements,[11,12,26] and femtosecond Raman induced Kerr effect spectroscopic (fs-RIKES) measurements[27] have been carried out in the last several years and each of these measurements indicated micro heterogeneous relaxation dynamics for the studied ionic DESs. Computer simulations have been carried out in recent times [7,28–30] to generate microscopic

understanding of the experimentally measured relaxation dynamics. Fluorescence based measurements among these studies have revealed fractional viscosity dependence for the measured solute rotational and translational timescales, and for the solvation energy relaxation timescales. Average dielectric relaxation times too showed fractional viscosity dependence, while the fs-RIKES experiments detected spectral signatures that were caused by the ion dependent microheterogeneity of these ionic DESs. Anomalous particle motions, such as, orientational[29] and translational[31] jumps have been detected in computer simulations and these might be recognised as heterogeneity markers for these media. Interestingly, these relatively more recent studies have essentially reconfirmed the micro heterogeneous nature of ionic DESs suggested already in several previous studies that reported ultrasonic and other measurements.[32–34]

Recent dielectric relaxation data accessed via measurements in a frequency window $0.2 \leq \nu/\mathrm{GHz} \leq 50$,[11,12] however, indicates a drastic difference between what has been registered now as electrolyte effects on the static dielectric constant (ε_s) of neat molten acetamide and what was concluded from earlier experiments carried out employing a frequency window, 0.1 Hz – 100 MHz.[34–38] More specifically, recent DR measurements in MHz-GHz frequency window have revealed ε_s ~20 – 30 for several ionic acetamide DESs. Considering ε_s ~ 70 for neat molten acetamide,[11] these values reflect substantial electrolyte-induced dielectric decrement of acetamide in these ionic DESs. This is in sharp contrast to the previous finding in Hz-MHz measurements which reported a colossal increase of the static dielectric constant ($\varepsilon_s \sim 10^6$) for ionic acetamide DESs that contained either NaSCN or CF_3COONa as an electrolyte. This mega-value of ε_s was then explained[34–36] in terms of 'charged locally ordered aggregates' formed by the host acetamide molecules and the electrolyte ions. These two conflicting DR data sets therefore trigger a debate on the true impact of electrolyte ions on the ε_s of the host acetamide, motivating further theoretical and/or experimental investigation employing different techniques for providing a resolution to this controversial issue. This forms the basis of the present work where we have used molecular dynamics simulations coupled with classical, coarse-grained model interaction potentials to monitor the time dependent fluctuations of the collective dipole moment of these ionic DESs. Our previous simulation study[39] of DR in neat molten acetamide employing the same model interaction potential acts as a supporting work to understand, at least, qualitatively the effects of ion on the rotational, translational and ro-translational contributions to the complex dielectric relaxation spectra

recorded in experiments. In this context we would like to mention that DR measurements of conducting media such as these ionic DESs in the low frequency wing is severely limited by one-over-frequency ($1/\omega$) divergence. Consequently, estimation of ε_s becomes tricky and often associates large error because of a large conductivity contribution in this frequency regime, inducing a rise in the real part of the complex dielectric spectrum and removing the usual plateau generated by the pure dipolar response alone. There exists indeed such a possibility for the previous Hz-MHz measurements,[34–36] whereas the more recent MHz-GHz experiments might have missed a certain portion of the low frequency response because of the limited coverage of the low frequency wing. Theoretical/computational studies do not suffer from these complexities and can successfully separate the dipolar and ionic components of the total frequency dependent DR spectrum.[40–42] Although this separation involves certain approximation, it offers the necessary framework that can deal with the ongoing controversy and provide a plausible resolution.

Dielectric relaxation spectroscopy (DRS) measures the collective polarization fluctuations of a given medium in the presence of a time dependent electric field.[43–46] The coupling between the frequency dependent electric field and the solvent polarization mode is assumed to be weak and linearly dependent on the fluctuating orientational density. Addition of electrolyte in pure dipolar solvent is known to increase or decrease the ε_s of neat solvents.[43,44,47–50] Formation of ion pair and other complex ionic species in weakly dipolar solvents, for example, lithium perchlorate in ethyl acetate is known to significantly increase the ε_s of the medium.[51–54] For uni-univalent electrolytes in strongly polar solvents, on the other hand, dielectric decrement can occur via static and kinetic routes. Static dielectric decrement occurs through a partial damage of the orientational order of the dipolar solvent molecules, while the kinetic decrement associates with the cross correlation between the dipole and ion density fluctuations[55,56] Fortunately, the underlying theoretical framework for computer simulations of the frequency dependent dielectric response of ionic media is available in the literature.[57,58] Dielectric response of aqueous solutions of uni-univalent electrolytes has been studied extensively via molecular dynamics simulations and these studies have provided important insights about the ion-induced impact on the frequency dependent dielectric response of aqueous media.[55,56,59–61] Frequency dependent dielectric spectra and conductivities of pure and aqueous solutions of ionic liquids have been investigated and ionic contributions to the total response have been separated.[40,62–67] These works have made important contributions to understand the interaction

and dynamics of ionic liquids revealed by dielectric relaxation experiments,[68–70] ultrafast fluorescence measurements[71–73] and theoretical calculations.[74–79]

In the present study, temperature-dependent simulations been performed in order to understand the effects of the ions on the DR of (CH_3CONH_2 + $LiClO_4$/ NO_3/ Br) DESs with a focus to generate a qualitatively correct description of electrolyte effects on the dielectric properties of the host acetamide which may help remove the ongoing debate initiated by the two different sets of DR measurements. Structural aspects have been explored by calculating the Kirkwood g factor and average number of H-bonds per acetamide molecule in these DESs. Dipolar and ionic components of the temperature dependent simulated dielectric relaxation spectra of these conducting media have been separated and the contributions of rotation-translation coupling to the total DR have been estimated. As expected, the dipolar contribution has been found to dominate the total DR spectrum. Anion dependent distribution of single dipole reorientation times do not indicate the presence of any unusually long timescale in these systems, whereas the average number of H-bonds per acetamide molecule shows a clear correlation with the ε_s estimated from the MHz-GHz DR measurements and from the present simulations.

II. SIMULATION DETAILS AND VALIDATION

Classical molecular dynamics simulations were performed using the GROMACS-2018.3 package[80] at four different temperatures, T(K) = 329, 336, 343, and 358. Acetamide molecules, cations and anions were taken in a ratio that mimicked the compositions employed in the MHz-GHz experiments. For each of the DESs considered, a total of 1000 particles (acetamide + cation + anion) were considered and the overall electroneutrality ensured. Composition of each system is given in **Table S1** (supplementary material). OPLS (optimized potentials for liquid simulations) type model force field were used[81]. Since the functional forms and notations associated with different pieces of the OPLS model potential were discussed earlier[39], these are provided in the **Appendix A1** (supplementary material). Interaction parameters developed[82] for correctly reproducing the experimental[83] ε_s of neat molten acetamide were employed to represent the acetamide molecules. The force-field parameters for Br^-, NO_3^-, and ClO_4^- were used as those available in the relevant literature[84]. Non-bonding parameters of Li^+ were taken from another work. [85] The cationic charge was scaled as 0.8e in order to be consistent with the anionic charges. Atomic representations of acetamide, cation and anions are shown in **Fig. S1** (supplementary material).

Initial cubic simulation boxes were constructed using the Packmol.[86] Leapfrog algorithm[87] along with a time-step of 2 fs was used for integrating the equation of motion. All bonds were kept constrained using the LINCS algorithm.[88] Non-bonded interactions were truncated at a cut-off distance of 1.1 nm. Temperature and pressure were coupled respectively to Nose-Hoover thermostat[89,90] and Parrinello-Rahman barostat [91,92] with coupling constants of 0.2 and 0.5 ps.

After energy minimization, each system was equilibrated in the NVT (10 ns) ensemble, followed by NPT equilibration for a period of another 10 ns. The equilibrated structure of the system thus obtained was further equilibrated in the NPT ensemble for another 60 ns. Subsequently, two production runs (NVT#1 and NVT#2) were performed. Among the three ionic deep eutectic systems, LiBr-DES is the most viscous one.[12] Therefore, comparatively longer simulation runs were performed for this DES. For the first NVT run (NVT#1), trajectories were saved in every 0.2 ps. This trajectory was used to calculate the rotational part of the dielectric relaxation spectra. For $LiClO_4$-DES, and $LiNO_3$-DES, these run spans were of 80 ns duration, while it was 130 ns for LiBr-DES. For each of these systems, 20 ns trajectories were saved at 0.02 ps time step (NVT#2) in order to better capture the short time dynamics.

Subsequently, the validity of the force field parameters was checked by comparing the simulated densities against those from experiments.[7,93] This comparison is shown in **Fig. S2** (supplementary material), while the numerical values are summarized in **Table S2** (supplementary material). Clearly, the deviation is <1% for $LiClO_4$-DES and $LiNO_3$-DES. For LiBr-DES, however, the agreement is poorer than this.

III. FREQUENCY-DEPENDENT DIELCTRIC FUNCTION: Connection to Experiments and Comparison

(a) Necessary Equations: A Brief Discussion

Dielectric relaxation spectroscopy is an important tool to investigate collective polarization fluctuation dynamics of a wide variety of complex systems.[45,46,94–97] Moreover, data from broadband DR measurements can explain the non-Markovian character of solvation response in complex systems that contain intermolecular H-bonding and ions.[98] The intimate relationship between DR and solvation response then identifies the molecular motions that dictates the progress of a chemical reaction and unravels the associated nature of the underlying microscopic friction. [99,100]

DR experiments, however, monitor the long wavelength ($k\sigma \to 0$, k and σ being the wavenumber and particle diameter respectively) polarization fluctuations and therefore microscopic lengthscale information on dynamics involving a few to several molecules is missing. Often a wide frequency range, covering several orders of magnitude, is required to measure the full dynamics and the measured response is then assigned rather qualitatively to collective solvent rotation and translation coupled rotation.[40,101] This is because DR experiments cannot separately measure the rotational and the translational solvent contributions and a measured relaxation time constant cannot be attributed cleanly to a particular type of molecular dynamics. This is where appropriate theoretical formalism and computations can contribute to separate the relative contributions from the total response. Fortunately, such a formalism for ionic systems is already available[41,57,58,65,102] and we discuss here the main equations.

The generalized expression for the frequency-dependent dielectric function can be written in terms of the Fourier–Laplace transform of the equilibrium total dipole moment of the system, $\boldsymbol{M}_{tot}$, as follows[41]

$$\Sigma(\omega) = \frac{1}{3\epsilon_0 V k_B T} \mathcal{L}\left[-\frac{d}{dt}\phi_{tot}(t)\right], \qquad (1)$$

where $\phi_{tot}(t) = \langle \boldsymbol{M}_{tot}(0) \cdot \boldsymbol{M}_{tot}(t) \rangle$. Note the time dependent collective dipole moment, $\boldsymbol{M}_{tot}(t)$, can be approximated as a sum of two independently fluctuating contributions, namely, the rotational ($\boldsymbol{M}_D$) and the translational ($\boldsymbol{M}_J$) components: $\boldsymbol{M}_{tot}(t) = \boldsymbol{M}_D(t) + \boldsymbol{M}_J(t)$.

The total collective dipole moment correlation function then takes the following form

$$\langle \boldsymbol{M}_{tot}(0).\boldsymbol{M}_{tot}(t) \rangle = \phi_{DD}(t) + \phi_{JJ}(t) + \phi_{DJ}(t), \qquad (2)$$

where $\phi_{DD}(t) = \langle \boldsymbol{M}_D(0).\boldsymbol{M}_D(t) \rangle$, $\phi_{JJ}(t) = \langle \boldsymbol{M}_J(0).\boldsymbol{M}_J(t) \rangle$ and $\phi_{DJ}(t) = \langle \boldsymbol{M}_D(0).\boldsymbol{M}_J(t) \rangle + \langle \boldsymbol{M}_J(0).\boldsymbol{M}_D(t) \rangle$ represent respectively the rotational, the translational and the ro-translational contributions. Laplace-Fourier transform of these separated out correlation

functions then provides the individual contributions to total frequency dependent dielectric function. They are defined as follows:

(i) rotational part, $\mathcal{L}\left[-\frac{d}{dt}\phi_{DD}(t)\right] = \langle \boldsymbol{M}_D^2 \rangle + i\omega\mathcal{L}_{DD}(\omega)$, (6)

(ii) translational part, $\mathcal{L}\left[-\frac{d}{dt}\phi_{JJ}(t)\right] = \frac{i}{\omega}\mathcal{L}_{JJ}(\omega)$, (7)

(iii) ro-translational part, $\mathcal{L}\left[-\frac{d}{dt}\phi_{DJ}(t)\right] = -2\mathcal{L}_{DJ}(\omega)$. (8)

In the above equations, $\mathcal{L}_{DD}(\omega) = \mathcal{L}[\langle \boldsymbol{M}_D(0).\boldsymbol{M}_D(t)\rangle]$, $\mathcal{L}_{JJ}(\omega) = \mathcal{L}[\langle \boldsymbol{J}(0).\boldsymbol{J}(t)\rangle]$ and $\mathcal{L}_{DJ}(\omega) = \mathcal{L}[\langle \boldsymbol{M_D}(0).\boldsymbol{J}(t)\rangle]$ where $\boldsymbol{J}(t) = \frac{d\boldsymbol{M}_J(t)}{dt}$.

The well-known $1/\omega$ divergence problem for conducting solutions at the low-frequency regime can be tackled in the present theoretical formalism by subtracting the zero-frequency contribution, $\mathcal{L}_{JJ}(\omega = 0)$, from the frequency dependent translational component, $\mathcal{L}_{JJ}(\omega)$.[41] This can be done by Laplace-Fourier transforming the equation required to fit the simulated $\langle \boldsymbol{J}(0).\boldsymbol{J}(t)\rangle$. Therefore, the calculated translational contribution is modified as $\Big(\mathcal{L}_{JJ}(\omega) - \mathcal{L}_{JJ}(0)\Big)$.

The individual contributions can then be obtained from the following relations,

(i) rotational spectra, $\varepsilon_{DD}(\omega) = \frac{1}{3\epsilon_0 V k_B T}\big(\langle \boldsymbol{M}_D^2 \rangle + i\omega\mathcal{L}_{DD}(\omega)\big)$, (9)

(ii) translational spectra, $\varepsilon_{JJ}(\omega) = \frac{1}{3\epsilon_0 V k_B T}\frac{i}{\omega}\Big(\mathcal{L}_{JJ}(\omega) - \mathcal{L}_{JJ}(0)\Big)$, (10)

(iii) ro-translational spectra, $\varepsilon_{DJ}(\omega) = \frac{1}{3\epsilon_0 V k_B T}\mathcal{L}_{DJ}(\omega)$. (11)

The conductivity-corrected generalized frequency dependent dielectric function, $\Sigma_0(\omega)$, is then expressed as follows[41]

$$\Sigma_0(\omega) = \Big(\varepsilon_{DD}(\omega) + \varepsilon_{JJ}(\omega) - 2\varepsilon_{DJ}(\omega)\Big). \quad (12)$$

Subsequently, the static dielectric constant is calculated as follows: $\varepsilon_s = \lim_{\omega \to 0} \left(\varepsilon_{DD}(\omega) + \varepsilon_{JJ}(\omega) - 2\varepsilon_{DJ}(\omega) \right) + 1$, while the dielectric constant at $\omega \to \infty$ is approximated as unity ($\varepsilon_\infty = 1$).

The detailed descriptions of the expressions for $\varepsilon_{DD}(\omega)$, $\varepsilon_{JJ}(\omega)$ and $\varepsilon_{DJ}(\omega)$ are provided in the Appendix A2 (supplementary material).

(b) Simulation Results: Decomposition of the DR Spectra

Fig. 1 presents the simulated normalised decays of the pure rotational component of the collective total dipole moment autocorrelation function, $\phi_{DD}^{N}(t) = \langle \boldsymbol{M}_D(0).\boldsymbol{M}_D(t) \rangle / \langle \boldsymbol{M}_D(0).\boldsymbol{M}_D(0) \rangle$, along with their multi-exponential fits for these three ionic DESs. Notice that data at four different temperatures are shown in this figure, while the corresponding fit parameters are summarised in **Table S3** (supplementary material). Temperature-induced faster dynamics reflected in **Fig. 1** arises from the temperature dependence of the medium viscosity. $\phi_{DD}^{N}(t)$ tracks the collective dipole reorientation dynamics and therefore these decays represent the rotational relaxation of the acetamide molecules in these three DESs.

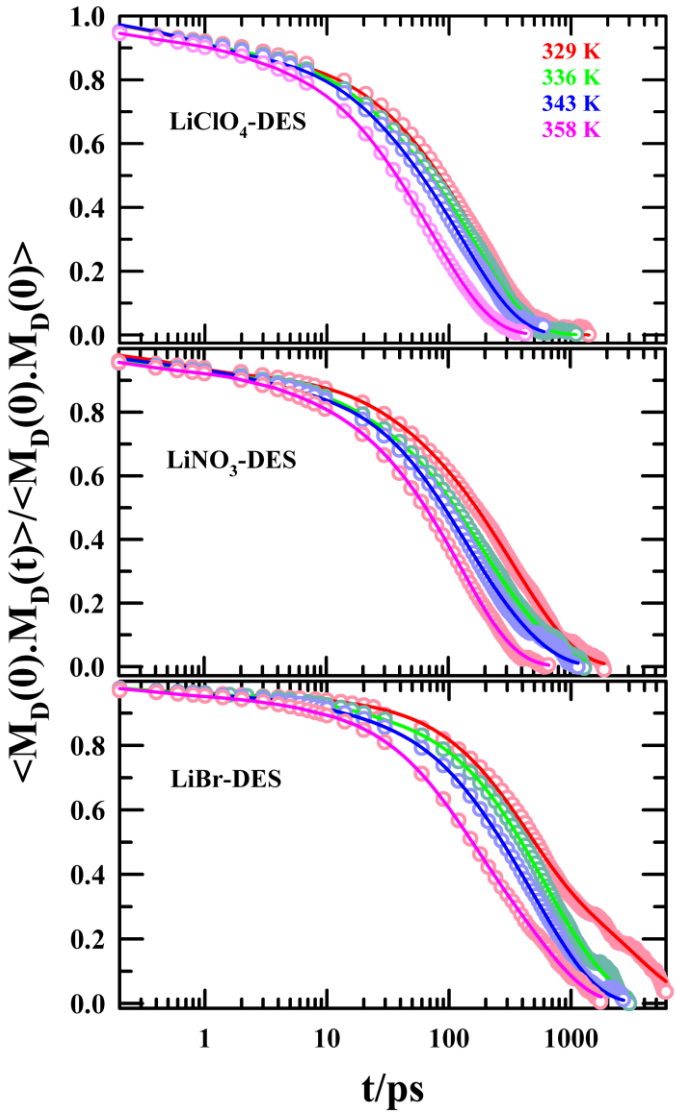

FIG. 1. Temperature-dependent decays of the normalised collective dipole moment autocorrelation function, $\phi_{DD}^{N}(t)$, simulated for the three ionic DESs considered in the present study. Open symbols represent the simulated data while the lines going through them denote the corresponding multi-exponential fits.

Fig. 2 displays the decay of the simulated current autocorrelation function, $\langle \boldsymbol{J}(0).\boldsymbol{J}(t)\rangle$ arising from ion translation, and relates to $\langle \boldsymbol{M}_J(0).\boldsymbol{M}_J(t)\rangle$ as follows. Because Laplace transform of the time derivative of $\langle \boldsymbol{M}_J(0).\boldsymbol{M}_J(t)\rangle$ enters into $\Sigma_0(\omega)$, we directly calculate $\boldsymbol{J}(t) = \frac{d}{dt}\left[\boldsymbol{M}_J(t)\right] = q.\frac{d}{dt}[\boldsymbol{r}(t)]$. Numerical fits through the data have also been presented in this figure, while fit functions and the associated fit parameters are provided in **Table S4** (supplementary material). The oscillatory behaviour with a dip at ~50 fs and a peak at ~100 fs arises from the decay behaviour of the underlying centre-of-mass velocity autocorrelation

function (VACF).[103] A very weak temperature dependence for these decays is registered. This is because the effects of temperature on VACF decay enter indirectly through the curvature of the potential energy surface generated by the nearest neighbour particles. For harmonic potential, force constant defines the curvature which does not depend on temperature explicitly.

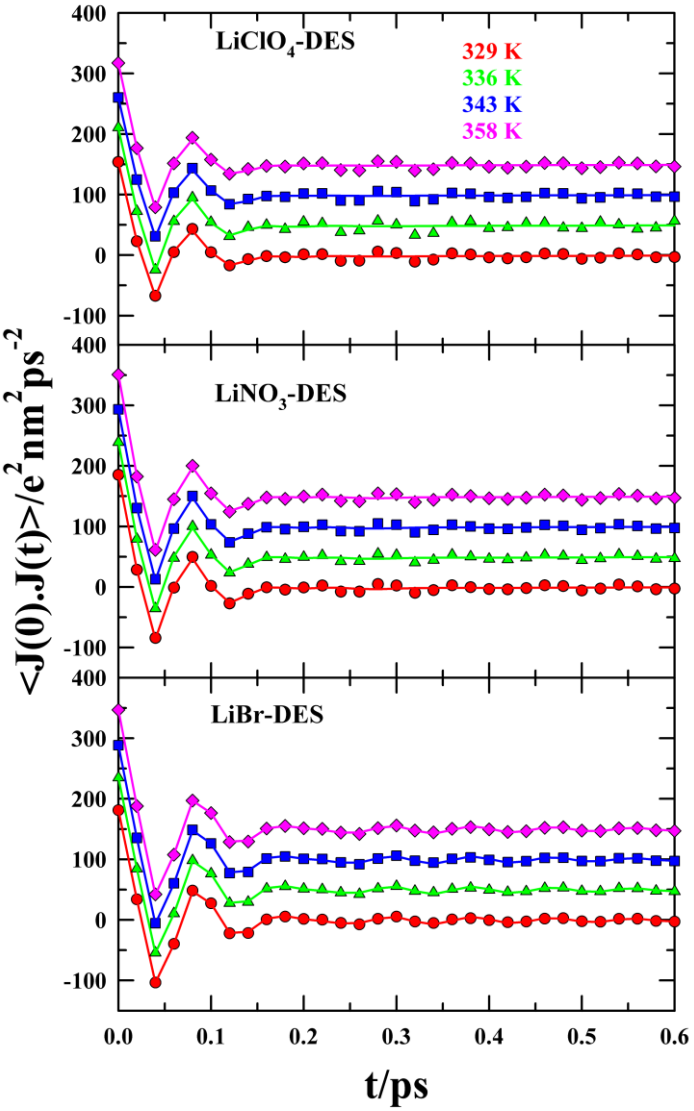

FIG. 2. Temperature-dependent decays of the current-current autocorrelation function for ions (cations and anions) in these three DESs. Closed symbols represent simulation data and solid lines going through them denote the corresponding fits. Note that an offset of 50 unit was used for a clear presentation of the temperature dependent curves.

We next present in **Fig. 3** the simulated dipole moment-current cross correlation functions for ions in these three DESs. These correlation functions are fitted numerically and the fit

parameters are shown in **Table S5** (supplementary material). This cross term is important because it embodies 'translation-rotation coupling' and contributes to both the frequency dependent permittivity and the conductivity. Note the nonmonotonic behaviour of this cross-correlation function with a peak at ~100 fs. This behaviour can be understood as follows. At $t = 0$, $\frac{dr}{dt} = v = 0$, and remembering that $\boldsymbol{J}(t) = \sum_{i(ion)} q_i \mathbf{v}_i(t)$, the numerical value of the cross-correlation function becomes zero. With time, the position vector of the particle ($\boldsymbol{r}(t)$) changes as well as its direction because of its interaction with the neighbouring particles. After a certain time, the direction vector assumes an orientation that might be parallel or near parallel to the projection of the collective dipole moment vector, $\boldsymbol{M}_{\mathrm{D}}(t = 0)$. This leads to the peak value of the cross-correlation function, $\langle \boldsymbol{M}_D(t = 0) \cdot \boldsymbol{J}(t) \rangle$. Subsequently, further interaction with the neighbours randomizes their relative orientation, leading to the decay of the correlation function. The temperature effect is negligible, although the cross-correlation contribution shows anion identity dependence and is the minimum for the LiBr containing DES which is the most viscous among the three systems considered. This highlights the important role played by the medium viscosity to facilitate translation-rotation decoupling.[104]

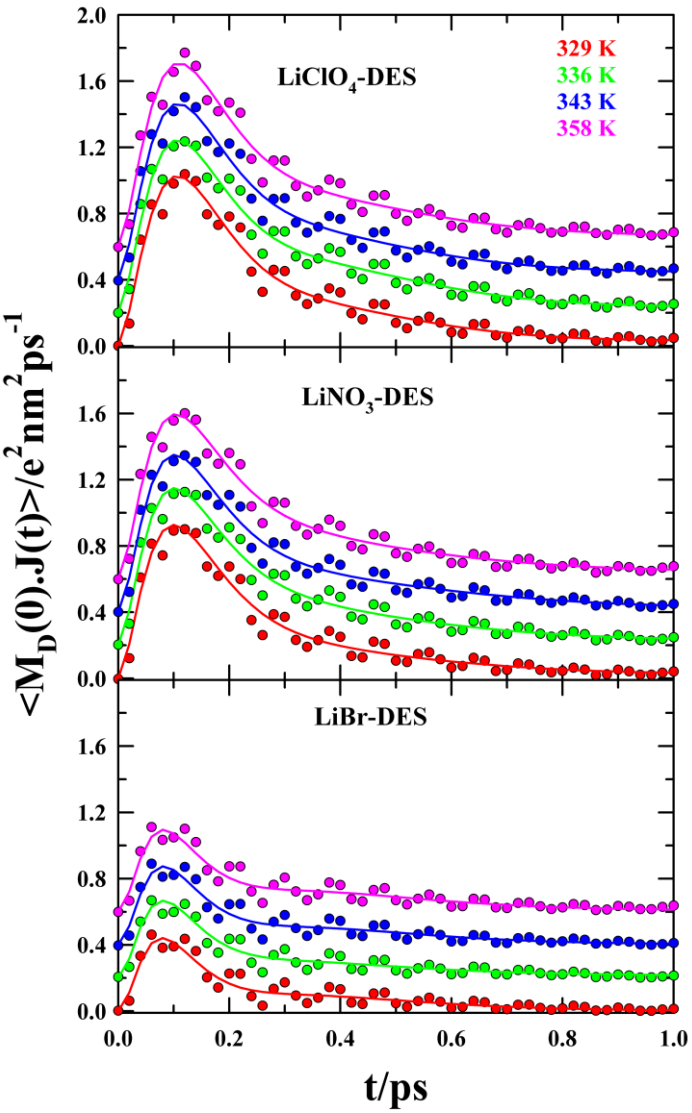

FIG. 3. Temperature-dependent dipole moment-current cross-correlation function for the three ionic acetamide DESs studied in this work. Closed symbols represent simulation data and solid lines going through them denote corresponding fits. Note that an offset of 0.2 unit was used for a clear presentation of the temperature dependent curves.

Laplace-Fourier transform of these three correlation functions generate rotational (ε_{DD}), translational (ε_{JJ}), and ro-translational (ε_{DJ}) contributions of the total dielectric spectra ($\Sigma_0(\omega)$) described by **Eq. 12**.

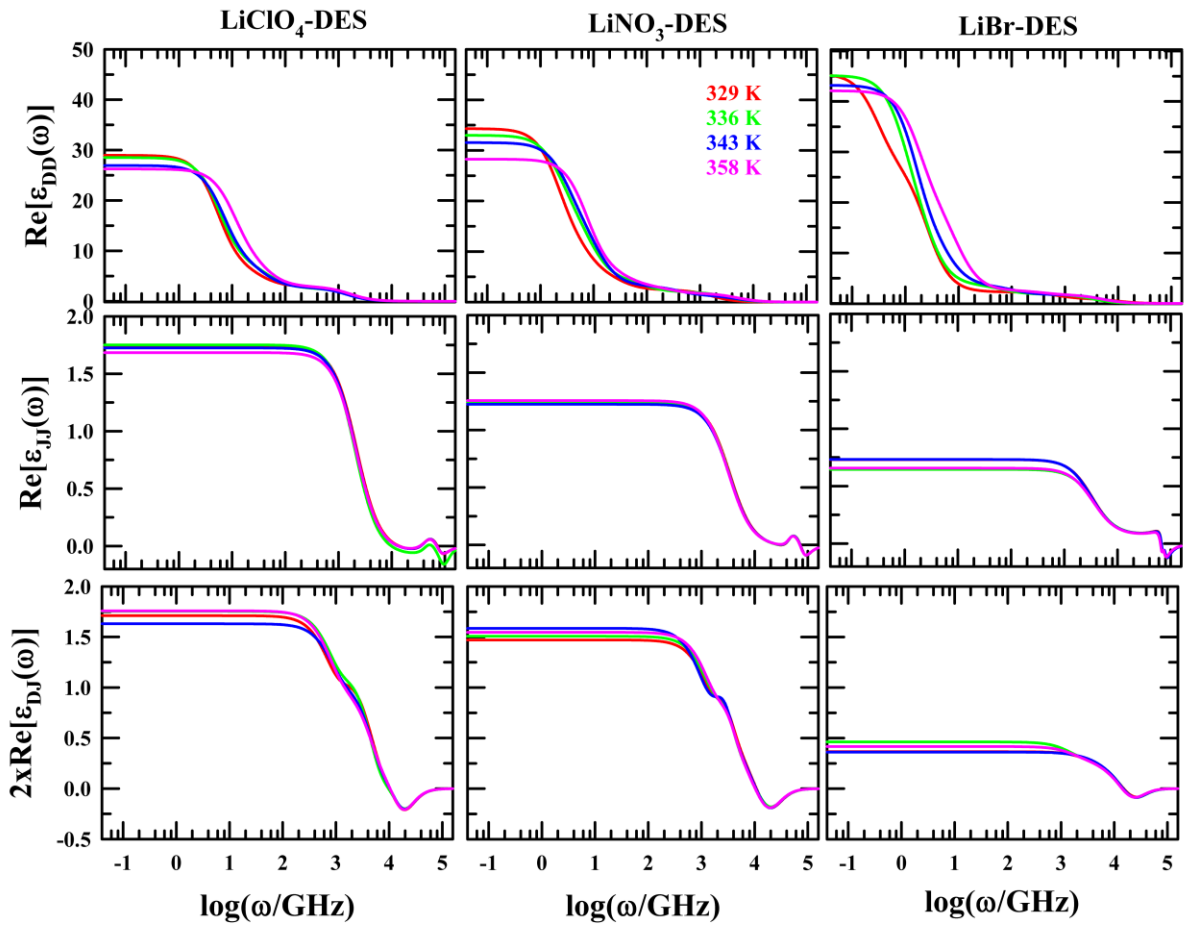

FIG. 4. Temperature-dependent real part of the dielectric spectra of the $LiClO_4$-DES (left), $LiNO_3$-DES (middle), and LiBr-DES (right): rotational spectra (upper), translational spectra (middle), ro-translational spectra (lower). Translational and ro-translational components are quite small compared to the rotational component.

Real and imaginary components of the rotational (ε_{DD}), translational (ε_{JJ}), and ro-translational (ε_{DJ}) contributions are presented in **Fig. 4** and **Fig. 5**, respectively. Numerical values of the real components of ε_{DD}, ε_{JJ}, and ε_{DJ} in the limit of zero frequency ($\omega \to 0$) are summarized in the last columns of **Tables S3-S5** of supplementary material.

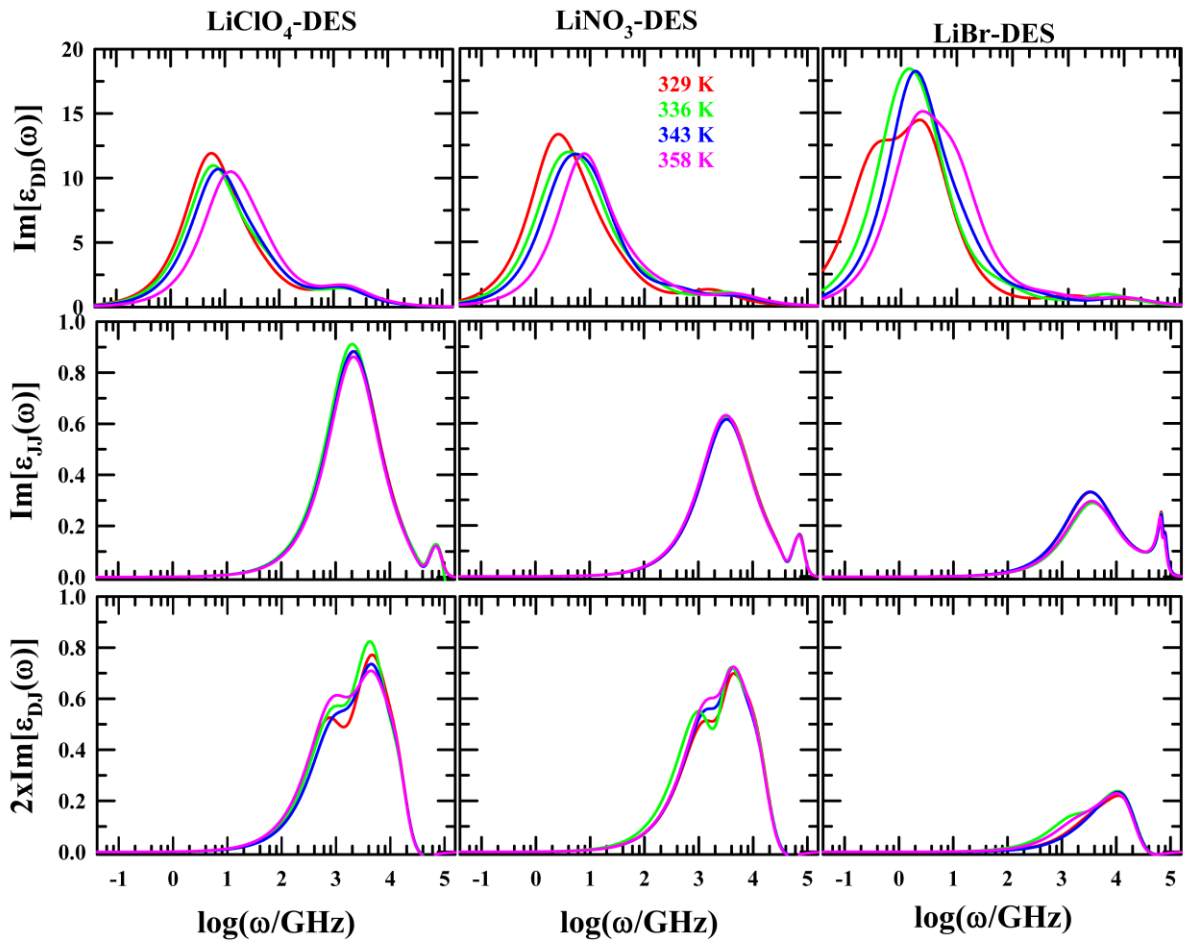

FIG. 5. Temperature-dependent imaginary part of the dielectric spectra of the $LiClO_4$-DES (left), $LiNO_3$-DES (middle), and LiBr-DES (right): rotational spectra (upper), translational spectra (middle), ro-translational spectra (lower). Notice the rotational relaxation occurs at the lower frequency wing while the translational and the ro-translational processes occur at the higher frequencies.

It is quite evident that ε_{DD} dominates the zero frequency values in all these ionic DESs, and the ro-translation contribution (cross term), found to be small magnitude and negative, reduces the overall value. In addition, these pieces reflect anion identity dependence. Subsequently, the real and the imaginary components of the frequency-dependent generalized dielectric function ($\Sigma_0(\omega)$), simulated at four different temperatures for these ionic DESs, are presented below in **Fig. 6**. As observed in experiments,[11,12] multi-Debye relaxation functions were found to adequately describe the simulated dielectric spectra. Moreover, temperature and anion identity dependencies are evident in simulations and parallel to those reported already in experimental studies.[11,12]

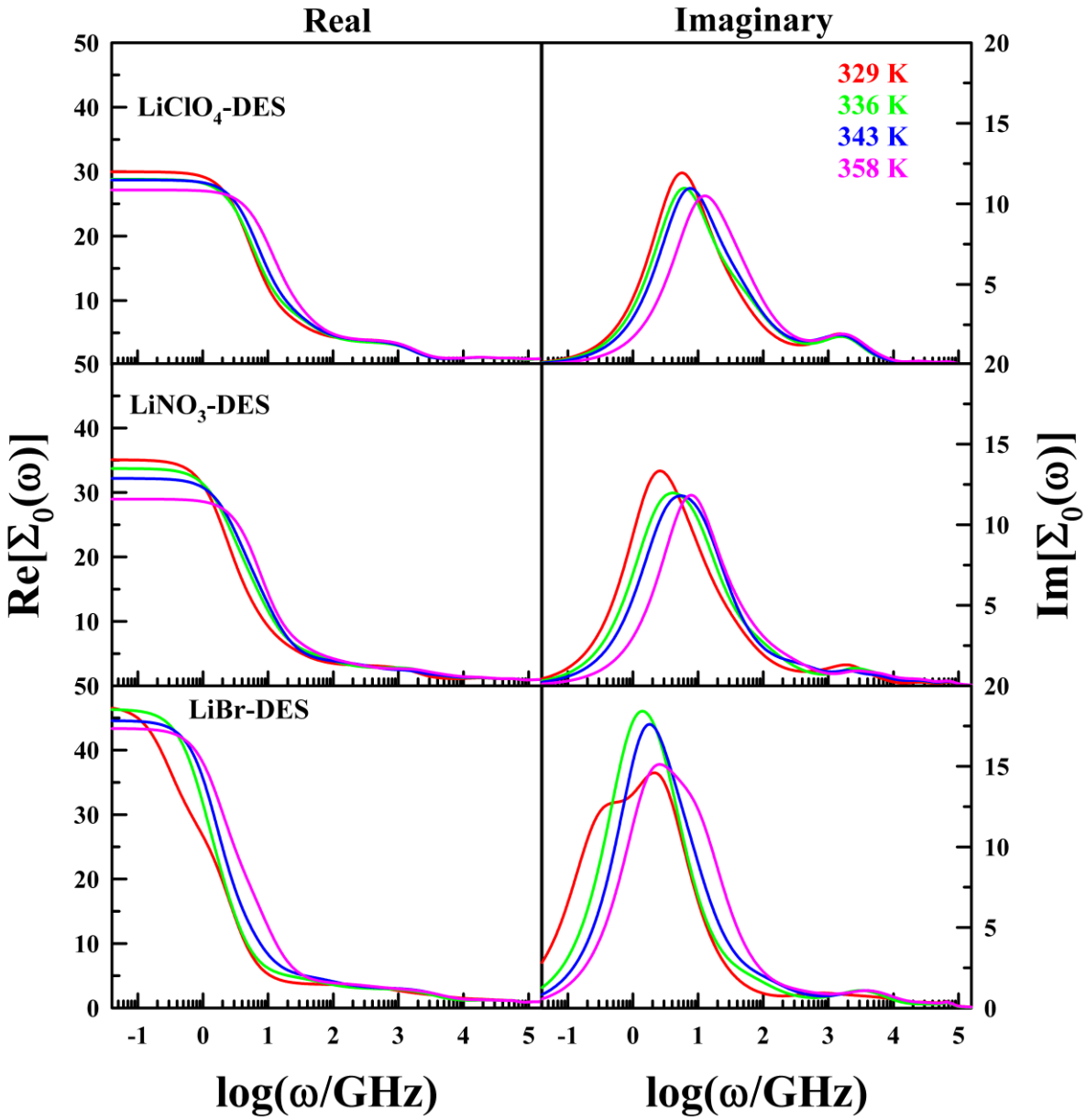

FIG. 6. Temperature-dependent real (left panel) and imaginary (right panel) components of the generalized frequency dependent dielectric function, $\Sigma_0(\omega)$, obtained from simulations via Eq. 12 of the text. Note that the peak of the imaginary component (lower panel) shifts to higher frequency (LiBr system being somewhat irregular) with temperature, whereas the zero-frequency value of the real component (left panel) modulates with anion identity. Effects of both temperature and electrolyte are quite evident in these figures.

The temperature dependent real and imaginary components of the simulated DR Spectra shown in **Fig. 6** required four Debye (4D) relaxation functions for simultaneous fits to describe

the DR processes in $LiNO_3$- and LiBr-DESs, whereas the $LiClO_4$-DES required three Debye (3D) relaxation functions. Numerical values of the temperature dependent relaxation time constants and amplitudes are summarized in **Table S3** (supplementary material). As we have already noticed the overwhelming dominance of the $\varepsilon_{DD}(\omega)$ over the other two contributions ($\varepsilon_{JJ}(\omega)$, and $\varepsilon_{DJ}(\omega)$) in determining $\Sigma_0(\omega)$, we consider the relaxation time constants from fits as arising from the medium dipolar response to the frequency dependent electric field. The temperature dependence of these multiple relaxation times is shown in **Fig. 7**. As expected, the temperature dependence is more pronounced for the relatively slower time constants (τ_1 and τ_2) and for systems with larger viscosities.[105]

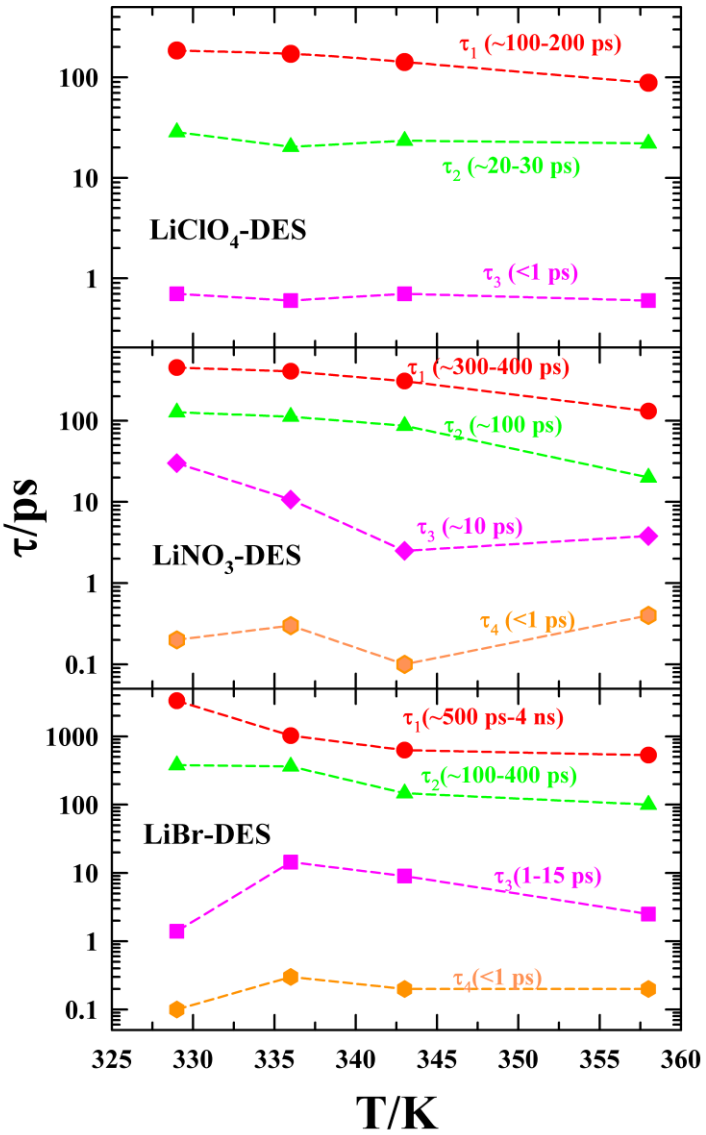

FIG. 7. Temperature-dependent DR time constants for the three DESs studied. The broken lines through the symbols are only guide to eyes. Viscosity (η) trend of these DESs are as follows: $\eta_{LiBr-DES} > \eta_{LiNO_3-DES} > \eta_{LiClO_4-DES}$.

Notice in **Fig. 7** the anion-dependence of the simulated DR time constants, particularly that of the relatively slower ones, τ_1 and τ_2. The slowest of the predicted DR time constants in these DESs follows the order, $\tau_{LiClO_4} < \tau_{LiNO_3} < \tau_{LiBr}$, and dictates the average DR time constant ($\langle\tau_{DR}\rangle = \sum_i a_i\tau_i$, with $\sum_i a_i$ =1) to follow the same trend. The origin and the dependencies (temperature and anion) of the experimentally measured DR time constants have already been discussed in terms of the structural hydrogen bond relaxation ($C_{HB}(t)$) and rank dependent single-particle reorientation dynamics ($C_\ell(t)$).[12] In **Table S6** (supplementary material) we have compared the simulated DR timescales with those from the structural hydrogen bond relaxation ($C_{HB}(t)$) and the first rank (ℓ =1) single-particle reorientation dynamics ($C_1(t)$).[12] This comparison re-establishes the already known interconnection among the DR dynamics, the structural H-bond fluctuations and the single particle reorientational relaxation.[28]

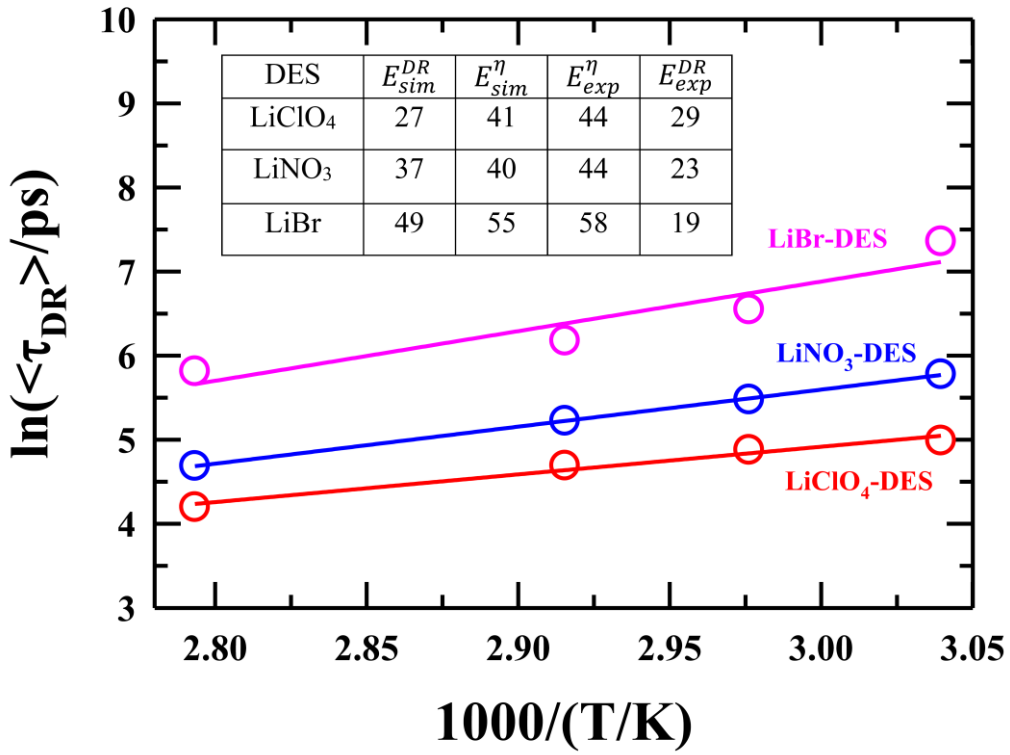

FIG. 8. Arrhenius type plot (ln ($\langle\tau_{DR}\rangle$) vs $^1/_T$) for three ionic DESs. Estimated activation energies are compared with those obtained from other dynamical processes. The values of

E_{sim}^{η} are taken from Ref. 105, and E_{exp}^{η} and E_{exp}^{DR} are from Ref. 12. Note that all values are rounded off to the nearest digit and in kJ/mol unit.

The effects of temperature on the simulated average DR times, $\langle \tau_{DR} \rangle$, is depicted in **Fig. 8**. A comparison among activation energies associated with DR times and viscosities obtained from simulations and experiments are also shown in the inset. Clearly, the anion dependent DR activation energies from simulations, E_{sim}^{DR}, follow the trend of viscosity activation energies from simulations and experiments, E_{sim}^{η} and E_{exp}^{η}, respectively. Interestingly, E_{sim}^{DR} does not follow the trend found in the experimental DR activation energies, E_{exp}^{DR}, although the simulated and experimental DR activation energies agree well for the lowest viscosity system, that is, perchlorate DES. The reason probably lies in the model interaction potential[82] employed that primarily focussed on optimizing the interaction parameters to reproduce the experimental static dielectric constant of the neat molten acetamide. This interaction potential has been found to overestimate the experimental DR times by a factor of ~2.[39] The simulated slower than experimental relaxation times fails to correctly describe the viscosity coupling of the diffusive dynamics, and as a result, the simulated DR activation energies show an anion dependence reverse of that found in measurements. An additional support to this view comes from a previous simulation study[105] which reported a much weaker decoupling between the centre-of-mass diffusion and viscosity than reported in experiments.

(c) Comparison with Experiments

We now compare our simulation results with those from DR measurements[12] performed employing the frequency window, $0.2 \leq \nu/GHz \leq 50$. Note that such a narrow frequency window can reliably measure DR dynamics with timescales ranging from a couple of picoseconds to a nanosecond only and therefore, faster and slower relaxations than these timescales will remain largely undetected. The present simulations do not suffer from such limitations. However, computer simulations are often sensitive to the accuracy of the model force field employed to mimic the interactions that govern the structure and dynamics of real systems and thus inherently limited to quantitatively reproduce experimental results. Here we have used a pair-wise additive classical force field which did not consider explicit description of polarizability.[82] The explicit description of polarizability and its systematic inclusion in

describing condensed phase systems, such as the present DESs where extensive inter-species H-bonding assumes a significant role, may become critically important. This is already reflected in the comparison between the simulated and the experimental DR activation energies presented in **Fig. 8**. This caveat notwithstanding, we persisted with this model interaction potential because the present study focuses on qualitatively correctly predicting electrolyte effects on the static dielectric constant of acetamide hosting these ionic DESs.

Fig. 9 compares the simulated and experimental static dielectric constants of these three DESs at two different temperatures. Clearly, the simulated dielectric constants agree well with those from the more recent MHz-GHz measurements[12] and sharply contrast the colossal increase found earlier in KHz-MHz experiments.[36–38] Also note in this figure that the agreement is better for systems with lower viscosities and follows the viscosity trend of these DESs. Numerical values of the DR parameters tabulated in **Tables S7-S9** (supplementary material) makes this comparison more quantitative.

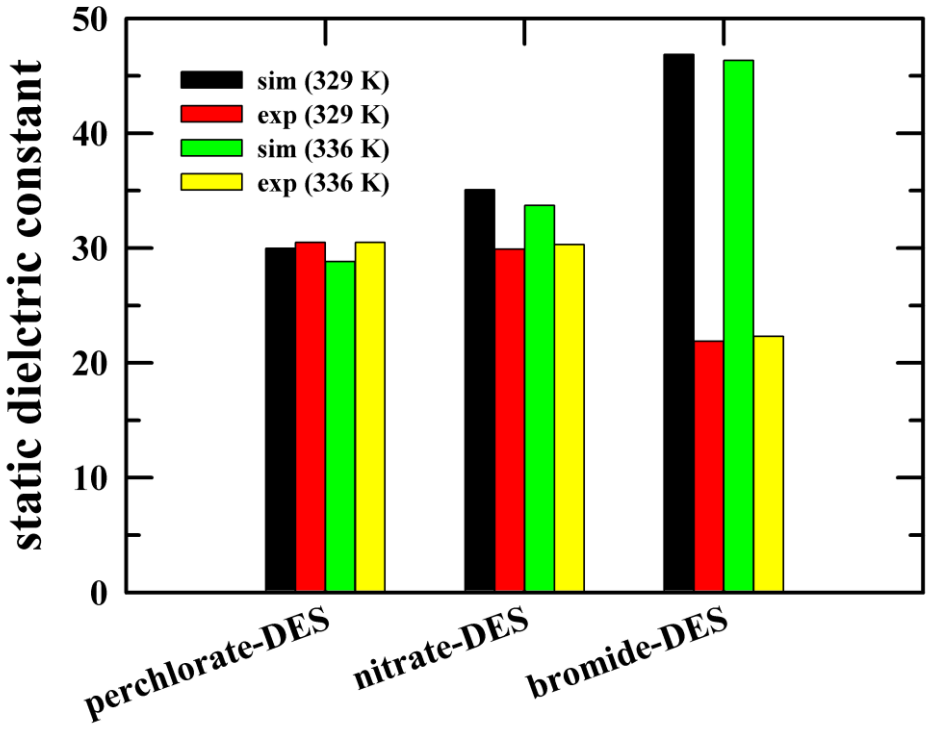

FIG. 9. Comparison of static dielectric constant values obtained from simulation and experiment for three ionic DESs at two temperatures.

Fig. 10 shows a comparison between the simulated and the experimental DR spectra for these three DESs at two different temperatures, 329 K and 336 K. Simulated and experimental

spectra (both the real and imaginary components) are presented after appropriate normalisation as follows: $(Re[\Sigma_0(\omega)] - \varepsilon_\infty)/(\varepsilon_s - \varepsilon_\infty)$ and $Im[\Sigma_0(\omega)]/(\varepsilon_s - \varepsilon_\infty)$. Reflecting the limitation of the model force field parameter, simulations predict relaxations slower than those recorded in experiments. The multi-Debye or non-Debye nature of the experimental dielectric relaxation is, however, correctly predicted in the present simulations.

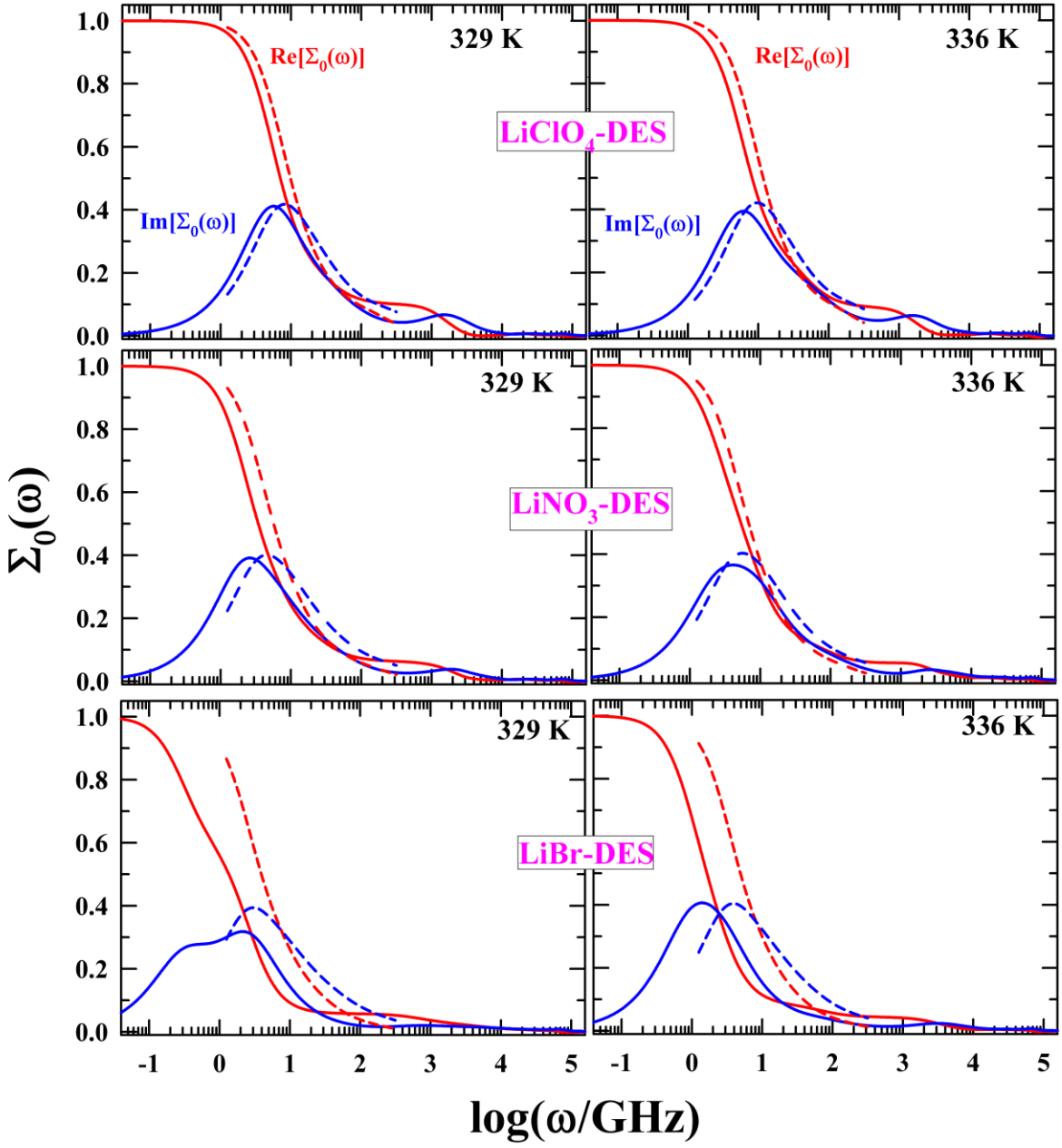

FIG. 10. Comparison between simulated and experimental dielectric spectra $LiClO_4$-DES (upper), $LiNO_3$-DES (middle), and LiBr-DES (lower). Real and imaginary components are indicated by red and blue, respectively. Results from simulations and experiments are denoted

by solid, and dashed lines, respectively. Experimental spectra are reproduced by using the fit parameters listed in Table 1 of **Ref. 12.**

The non-Debye (or multi-Debye) nature of DR can be confirmed via the Cole-Cole plot which, for a liquid with single Debye relaxation, describes a *perfect* semi-circle when the imaginary component is shown as a function of the real component of the frequency dependent DR spectrum. **Fig. 11** presents the Cole-Cole plots by using the real and imaginary components of the simulated DR spectra for these three DESs at two different temperatures. The non-Debye feature of the simulated spectra is clearly visible and more prominent for the bromide system. Notice in this figure that the non-Debye feature is not as prominent in the measured spectra as found in the simulations, and this may be partly due to the model force field parameters and partly due to the narrow frequency window employed in the relevant experiments. The non-Debye features however, subtle or prominent, justifies the requirement of multi-Debye fit functions for describing both the simulated and experimental DR spectra of these ionic DESs.

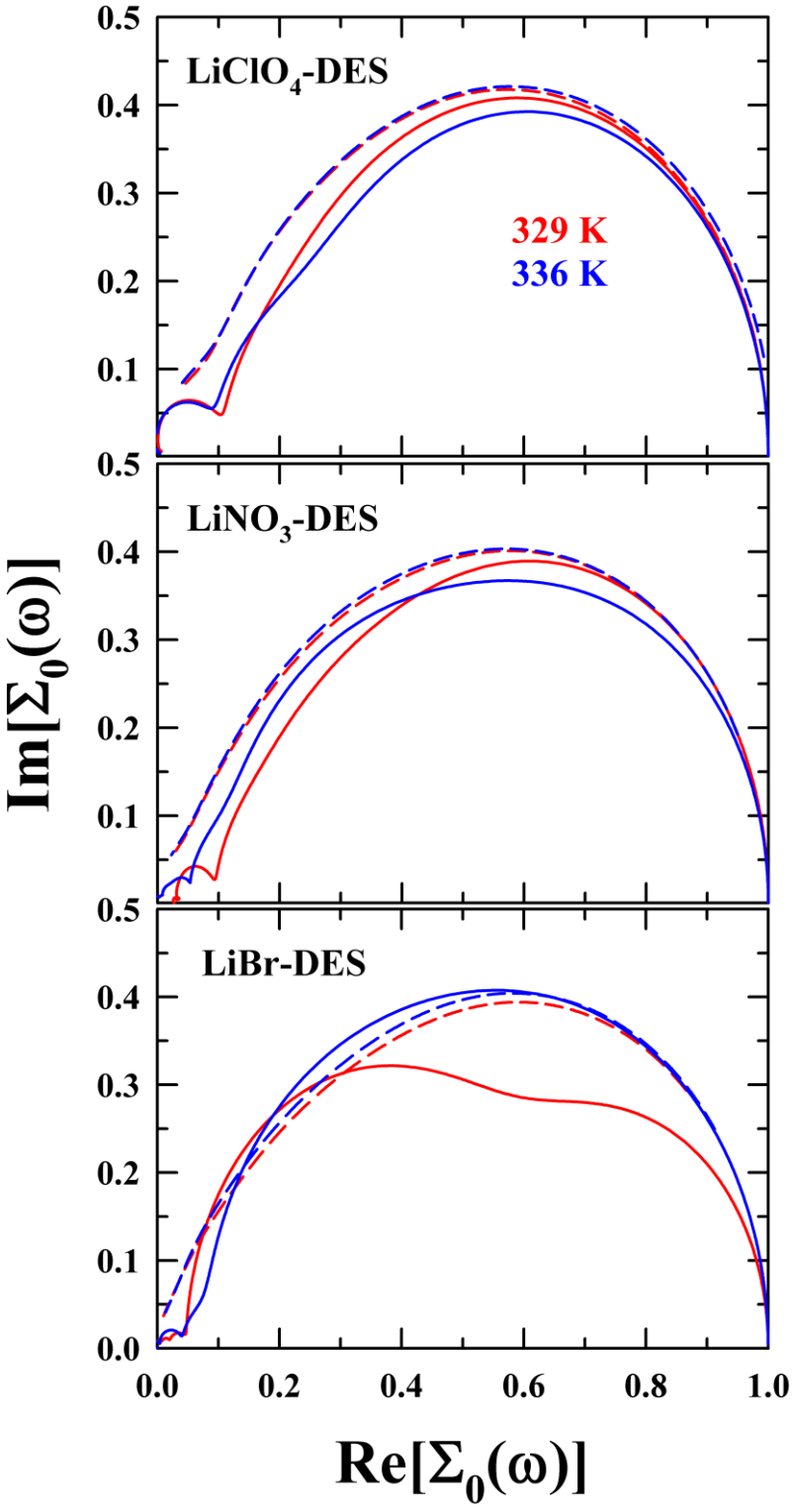

FIG. 11. Cole-Cole plots showing the non-Debye features in the DR spectra of the three DESs studied here. Simulated and measured spectra are represented respectively by the solid and the dashed lines.

IV. Dielectric Constant (ε_s) Decrement: Probable Reasons

Experiments carried out in recent times employing MHz-GHz frequency window have repeatedly shown substantial decrease in the value of the static dielectric constant (ε_s) of neat molten acetamide in DESs made of acetamide and uni-univalent electrolytes.[12] This electrolyte-induced decrease of ε_s or dielectric decrement is in sharp contrast to earlier reports based on KHz-MHz measurements[33,34,36–38] and thus warrants a closer scrutiny. Temperature-dependent simulated ε_s values for the three ionic acetamide DESs are shown via a bar chart in **Fig. 12** along with that for the neat molten acetamide. Clearly, ε_s values for the ionic acetamide DESs investigated are considerably lower than that of the neat molten acetamide, and shows dependence on both temperature and anion-identity. The phenomenon of the ion-induced dielectric decrement is, however, not new and has already been observed for conventional ionic solutions in both experiments[48–50,106,107] and simulations.[55,56,59–61,102,108–110] Traditionally, this has been explained considering two different scenarios. In the dynamic picture, solvent molecules in the first solvation shell are assumed to electrostatically bind with ions in solutions so comprehensively that those solvent molecules lose their orientational freedom and remain non-responsive to the frequency dependent electric field administered during DR measurements. This makes these *bound* solvent molecules to appear as *rotationally frozen* and cannot contribute to the frequency dependent dielectric function. The resultant decrease in ε_s is then termed as the kinetic dielectric decrement.[55,56]

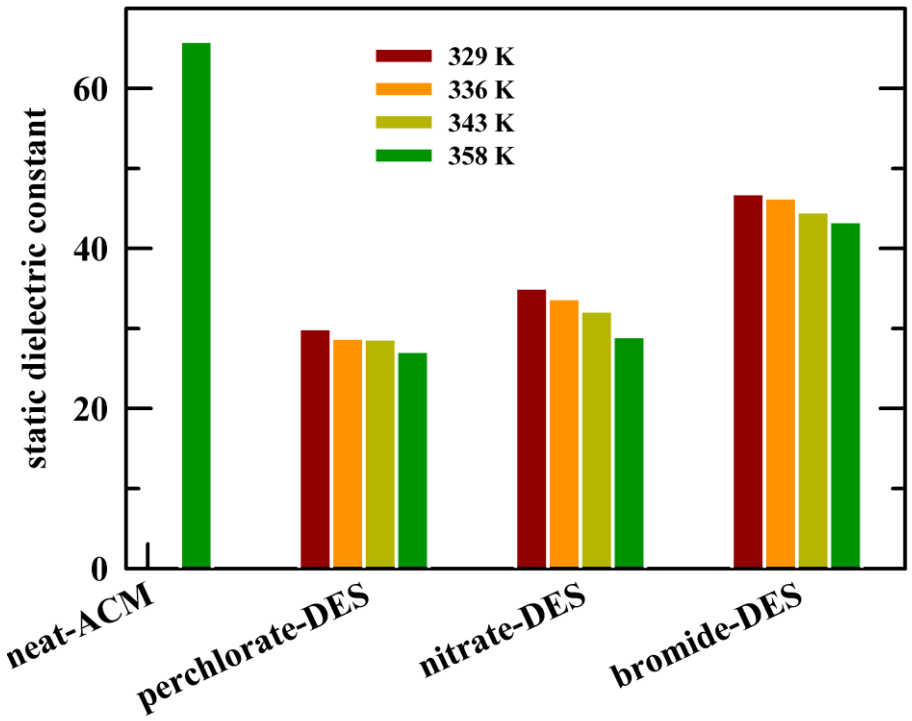

FIG. 12 Temperature-dependent static dielectric constant for three DESs. ε_s for liquid acetamide at 358 K is also shown for comparison. Each plot is color-coded.

The other origin, being static in nature, associates with the frustrations in the static orientational correlations among the solvent dipoles. This is important for network solvents such as water where the three-dimensional H-bond network forces the molecular dipoles to orient favourably, producing a high value for the Kirkwood g factor ($g_K \approx 3.7$) in the liquid phase.[111] The Kirkwood factor (G_k) estimates the dipolar correlations and is defined as,[112]

$$G_k = \frac{\langle|\boldsymbol{M}(0)|^2\rangle - \langle|\boldsymbol{M}(0)|\rangle^2}{N\mu^2} \quad , \qquad (13)$$

where the numerator denotes the variance of the total dipole moment of the system, N the number of dipoles present in a given system, and μ the average value of the dipole moment.

Fig. 13 presents the simulated G_k values for the three DESs and for the neat molten acetamide. The results are shown as a function of time in order to highlight the respective time evolutions and the fluctuations over time. A significant decrease in the value of G_k for each of these DESs

over that for the neat molten acetamide is clearly visible. This in turn reflects loss of orientational order among the molecular dipoles (acetamide molecules) in these DESs relative to that in neat molten acetamide. In addition, the extent of decrease depends on the identity of the anion. More specifically, the disruption of the static dipolar correlations is the most severe for the perchlorate ion among the three anions of the lithium salts considered. Note the simulated ε_s values shown in **Fig. 12** also follows the same trend and the connection arises because both G_k and ε_s depend upon the extent of dipolar correlations present in a given system.

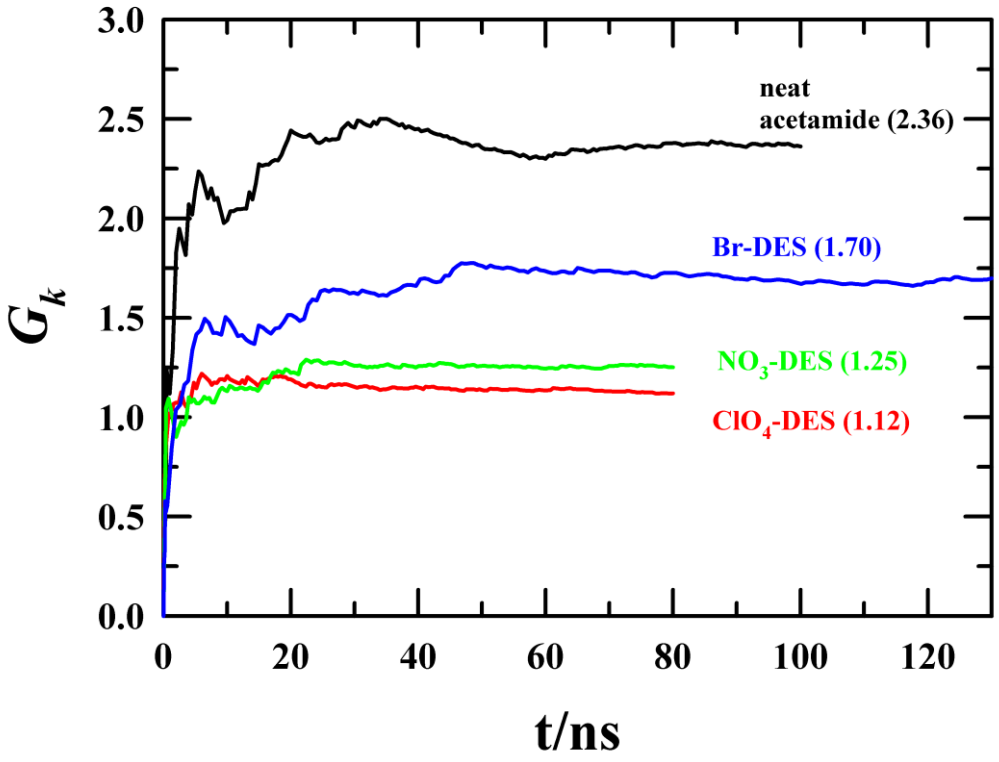

FIG. 13. Time evolution of the Kirkwood correlation factor (G_k) during simulations for pure acetamide and the three ionic acetamide DESs at 358 K. Time averaged values for G_k are shown in parentheses.

As already mentioned, intermolecular H-bond network critically influences the relative arrangements of molecular dipoles in space (dipolar correlations) and thus loss of dipolar correlations must accompany frustrations in the intermolecular H-bond network. We have therefore examined the H-bond network of acetamide in these DESs by calculating the average number of H-bonds per acetamide molecules in these DESs and in the neat molten acetamide.

The calculation procedure is available in the literature[29,113] and briefly discussed in the supplementary material (**Appendix A3**). **Fig. 14** shows the temperature dependent average number of H-bonds per acetamide molecule, $\langle n_{HB} \rangle$, in these three DESs. The same for the neat molten acetamide at 358 K is also shown for a qualitative comparison. Clearly, $\langle n_{HB} \rangle$ is substantially lower in these ionic DESs than that in the neat molten acetamide and exhibits an appreciable anion identity dependence. The mild temperature dependence of $\langle n_{HB} \rangle$ reflected here can be explained in terms of the relatively weaker temperature-induced randomization of the dipolar correlations. The same trend followed by the anion dependent ε_s, G_k and $\langle n_{HB} \rangle$ only highlights the fact that the dielectric decrement in the DESs is caused largely, if not solely, by the anion-induced damage of the intermolecular H-bond network among the host acetamide molecules, followed by the subsequent frustrations in the static dipolar correlations.

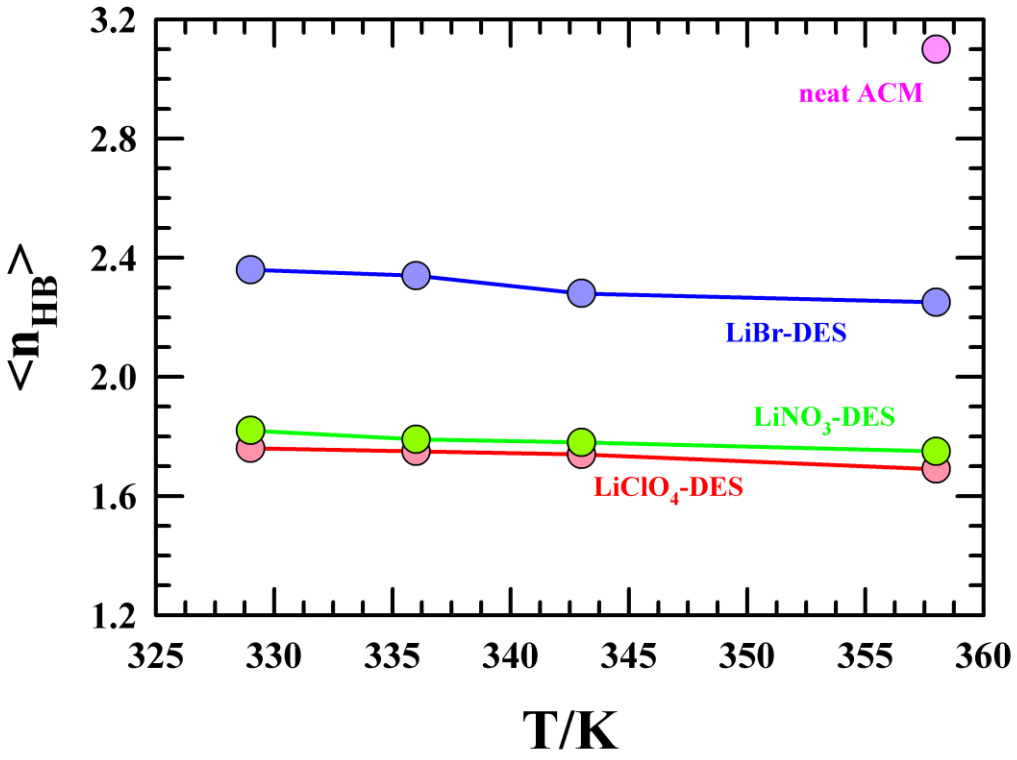

FIG. 14. Average number of hydrogen bonds per acetamide molecule, $\langle n_{HB} \rangle$, are shown for neat molten acetamide, and three ionic DESs studied. For ionic DESs, temperature-dependence of $\langle n_{HB} \rangle$ are shown. The solid lines going through the symbols act as guides to bare eye.

Next, we examine the presence of extremely slow 'irrotationally bound' acetamide molecules in order to understand the dynamic contribution to the observed ion-induced dielectric

decrement. For this, we have simulated the time averaged reorientation times ($\tau_{\boldsymbol{\mu}}$) for every single molecular dipole (acetamide molecule) present in the system by monitoring the following normalised time correlation function, $\phi_{\boldsymbol{\mu}}(t) = \frac{\langle \boldsymbol{\mu}(0).\boldsymbol{\mu}(t) \rangle}{\langle \boldsymbol{\mu}(0).\boldsymbol{\mu}(0) \rangle}$, with $\tau_{\boldsymbol{\mu}} = \int \phi_{\boldsymbol{\mu}}(t)dt$. We therefore obtained ~800 decay functions for each DES and those many individual $\tau_{\boldsymbol{\mu}}$ values.

The distributions of these individual relaxation times, $P(\tau_{\mu})$, for these three ionic DESs are presented in **Fig. 15.** Interestingly, although LiBr-DES shows the most sluggish reorientation dynamics, the slowest time is limited to a few ns. This confirms the absence of 'irrotationally bound' extremely slow acetamide molecules in these model DES systems, lowering the possibility for the dynamics to contribute to the observed dielectric decrement.

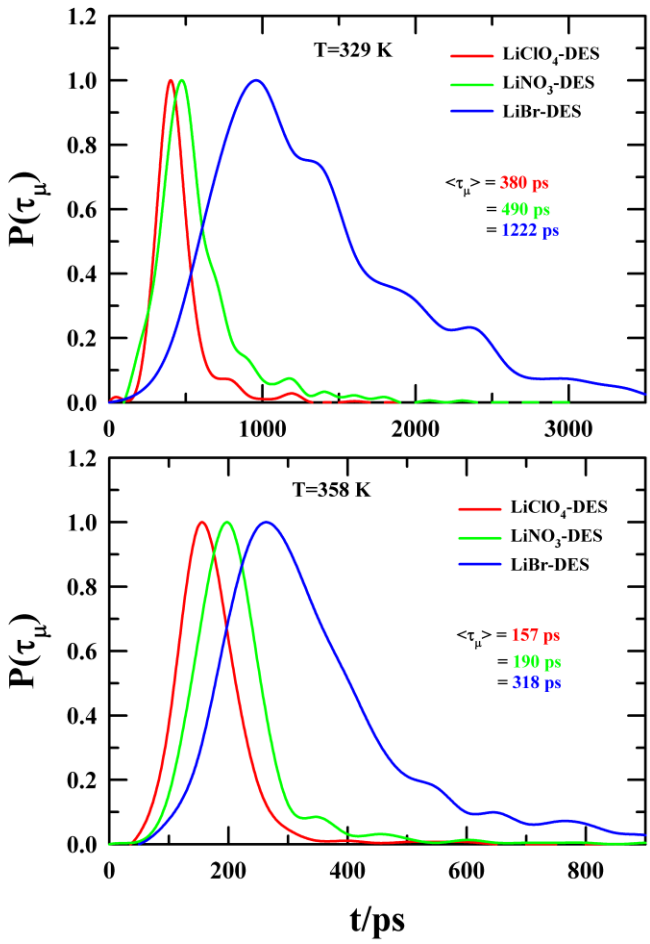

FIG. 15. Normalised probability distributions, $P(\tau_{\mu})$, of single-dipole orientation times in the three ionic DESs at 329 K (upper panel), and 358 K (lower panel).

VI. CONCLUSION

To summarize, a thorough temperature dependent simulation study of dielectric relaxation in (acetamide + lithium perchlorate/ nitrate/ bromide) deep eutectics has been carried out to understand the effects of electrolyte on the dielectric behaviour of these systems. This has been done by separating out the dipole rotational, ion translational and the coupled dipole-ion ro-translational contributions that constitute the total frequency dependent dielectric function. The dipolar (rotational) contribution has been found to overwhelmingly dominate the DR spectra at all the temperatures considered, while the other two contributions are quite small. A comparison with the available experimental data indicates that the impact of the electrolyte on the static dielectric constant has been predicted successfully by the present simulations, although the simulated relaxations times have been overestimated by approximately a factor of 2. This is mainly due to the inherent nature of the force field employed to represent acetamide in this work. A novel finding of this study is the prediction of ion-induced decrement of the static dielectric constant of these DESs and its (the decrement) dependence on the identity of the anion. Further investigation suggest that this decrement is arising from the partial randomization of the dipolar correlations that accompanies substantial frustrations in the acetamide H-bonding network. Our analyses indicate that the decrement is largely static in nature because the simulated distributions of the individual dipole rotation times do not predict rotation times beyond a few nanoseconds. This is a new insight to the DR behaviour of these ionic DESs and these findings explain the recent MHz-GHz DR measurements in microscopic terms. Importantly, this simulation study provides a resolution to a long-standing debate on the actual impact of electrolytes on the static dielectric constant of acetamide in these ionic DESs.

We would like to mention that the present study could not successfully predict the experimental trend of the anion dependent DR activation energy. More precisely, these simulations have failed to predict correctly the extent of viscosity decoupling found for average DR time constants in the bromide DES. As we have already mentioned, this failure is because of the inherent limitations of the model force field parameters. Our initial study employing different force field (OPLS-AA) parameters[114] for acetamide predicted weak anion dependence of both the static dielectric constant and relaxation times (results not shown). The development of a new force field describing correctly both the experimental dielectric constant and the relaxation times for molten acetamide might be an important problem for future study.

SUPPLEMENTARY MATERIAL

The supplementary material contains Number of constituent particles in the three DESs, functional form of the OPLS potential model, atomic representations of DES molecules, comparison between temperature-dependent simulated and measured densities of DESs, brief description of calculating dielectric spectra from simulation trajectory, fit parameters for rotational, translational and ro-translational correlation functions at different temperatures, temperature-dependent multi-exponential fit parameters for the simulated $C_{HB}(t)$, $C_1(t)$, and DR timescales, Comparison between static dielectric constant and dielectric relaxation times obtained from simulation and experiments for three the DESs, analysis protocol to calculate number of hydrogen bonds.

ACKNOWLEDGEMENT

DM acknowledges DST-INSPIRE, Govt. of India for providing research fellowship.

DATA AVAILABILITY

The data that support the findings of this study are available from the corresponding author upon reasonable request.

AUTHOR DECLARATIONS

Conflict of interest

The authors have no conflicts to disclose.

Author Contributions

DM carried out the simulations, analysed the data, participated in discussion, and wrote the paper. RB arranged the necessary resources, chose the problem, supervised the work, analysed the simulated data, and worked on the successive drafts to finalize the manuscript.

References

[1] Q. Zhang, K. de Oliveira Vigier, S. Royer, and F. Jérôme, Chem Soc Rev **41**, 7108 (2012).

[2] E.L. Smith, A.P. Abbott, and K.S. Ryder, Chem Rev **114**, 11060 (2014).

[3] P. Xu, G.-W. Zheng, M.-H. Zong, N. Li, and W.-Y. Lou, Bioresour Bioprocess **4**, 34 (2017).

[4] R. Svigelj, N. Dossi, C. Grazioli, and R. Toniolo, Sensors **21**, 4263 (2021).

[5] P. Atkins, J. de Paula, and J. Keeler, *Atkins' Physical Chemistry*, 11th ed. (Oxford University Press, 2017).

[6] B. Guchhait, S. Daschakraborty, and R. Biswas, J. Chem. Phys. **136**, 174503 (2012).

[7] B. Guchhait, S. Das, S. Daschakraborty, and R. Biswas, J. Chem. Phys. **140**, 104514 (2014).

[8] B. Guchhait, H. al Rasid Gazi, H.K. Kashyap, and R. Biswas, J. Phys. Chem. B **114**, 5066 (2010).

[9] S. Dinda, A. Sil, A. Das, E. Tarif, and R. Biswas, J Mol Liq **349**, 118126 (2022).

[10] N. Subba, E. Tarif, P. Sen, and R. Biswas, J Phys Chem B **124**, 1995 (2020).

[11] K. Mukherjee, A. Das, S. Choudhury, A. Barman, and R. Biswas, J. Phys. Chem. B **119**, 8063 (2015).

[12] K. Mukherjee, S. Das, J. Rajbangshi, E. Tarif, A. Barman, and R. Biswas, J. Phys. Chem. B **125**, 12552 (2021).

[13] Y. Dai, J. van Spronsen, G.-J. Witkamp, R. Verpoorte, and Y.H. Choi, J. Nat. Prod. **76**, 2162 (2013).

[14] G. García, S. Aparicio, R. Ullah, and M. Atilhan, Energy & Fuels **29**, 2616 (2015).

[15] M. Sharma, C. Mukesh, D. Mondal, and K. Prasad, RSC Adv **3**, 18149 (2013).

[16] S. Handy and K. Lavender, Tetrahedron Lett. **54**, 4377 (2013).

[17] O.E. Geiculescu, D.D. Desmarteau, S.E. Creager, O. Haik, D. Hirshberg, Y. Shilina, E. Zinigrad, M.D. Levi, D. Aurbach, and I.C. Halalay, J. Power Sources **307**, 519 (2016).

[18] V. Lesch, A. Heuer, B.R. Rad, M. Winter, and J. Smiatek, Phys. Chem. Chem. Phys. **18**, 28403 (2016).

[19] E.L. Smith, A.P. Abbott, and K.S. Ryder, Chem. Rev. **114**, 11060 (2014).

[20] C. D'Agostino, R.C. Harris, A.P. Abbott, L.F. Gladden, and M.D. Mantle, Phys. Chem. Chem. Phys. **13**, 21383 (2011).

[21] A.P. Abbott, G. Capper, and S. Gray, ChemPhysChem **7**, 803 (2006).

[22] A.P. Abbott, J.C. Barron, K.S. Ryder, and D. Wilson, Chem. - Eur. J. **13**, 6495 (2007).

[23] B. Guchhait, S. Das, S. Daschakraborty, and R. Biswas, J. Chem. Phys. **140**, 104514 (2014).

[24] A. Das, S. Das, and R. Biswas, Chem. Phys. Lett. **581**, 47 (2013).

[25] A. Das, S. Das, and R. Biswas, J. Chem. Phys. **142**, 034505 (2015).

[26] S.N. Tripathy, Z. Wojnarowska, J. Knapik, H. Shirota, R. Biswas, and M. Paluch, J. Chem. Phys. **142**, 184504 (2015).

[27] R. Biswas, A. Das, and H. Shirota, J. Chem. Phys. **141**, 134506 (2014).

[28] S. Das, R. Biswas, and B. Mukherjee, J. Chem. Phys. **145**, 084504 (2016).

[29] S. Das, R. Biswas, and B. Mukherjee, J. Phys. Chem. B **119**, 11157 (2015).

[30] T. Pal and R. Biswas, Chem. Phys. Lett. **517**, 180 (2011).

[31] S. Banerjee, P.Kr. Ghorai, D. Maji, and R. Biswas, J Phys Chem B **126**, 10146 (2022).

[32] D.J. Mitchell and B.W. Ninham, Journal of the Chemical Society, Faraday Transactions 2 **77**, 601 (1981).

[33] G. Berchiesi, G. Vitali, P. Passamonti, and R. Płowiec, J. Chem. Soc., Faraday Trans. 2 **79**, 1257 (1983).

[34] G. Berchiesi, J Mol Liq **83**, 271 (1999).

[35] D.C. Prieve and R. Roman, Journal of the Chemical Society, Faraday Transactions 2 **83**, 1287 (1987).

[36] G. Berchiesi, F. Farhat, M. de Angelis, and S. Barocci, J Mol Liq **54**, 103 (1992).

[37] A. Amico, G. Berchiesi, C. Cametti, and A. di Biasio, J. Chem. Soc., Faraday Trans. 2 **83**, 619 (1987).

[38] G. Berchiesi, M. de Angelis, G. Rafaiani, and G. Vitali, J Mol Liq **51**, 11 (1992).

[39] D. Maji, S. Indra, and R. Biswas, J Chem Sci **133**, 1 (2021).

[40] C. Schröder, J. Hunger, A. Stoppa, R. Buchner, and O. Steinhauser, J. Chem. Phys. **129**, 184501 (2008).

[41] C. Schröder and O. Steinhauser, J Chem Phys **132**, 244109 (2010).

[42] M. Schmollngruber, D. Braun, and O. Steinhauser, J. Chem. Phys. **145**, (2016).

[43] R. Buchner, Pure and Applied Chemistry **80**, 1239 (2008).

[44] R. Buchner and J. Barthel, Annual Reports Section "C" (Physical Chemistry) **91**, 71 (1994).

[45] H. Weingärtner, P. Sasisanker, C. Daguenet, P.J. Dyson, I. Krossing, J.M. Slattery, and T. Schubert, J. Phys. Chem. B **111**, 4775 (2007).

[46] C. Schröder, C. Wakai, H. Weingärtner, and O. Steinhauser, J. Chem. Phys. **126**, (2007).

[47] R. Buchner, G.T. Hefter, and P.M. May, J. Phys. Chem. A **103**, 1 (1999).

[48] R. Buchner and G. Hefter, Phys. Chem. Chem. Phys. **11**, 8984 (2009).

[49] T. Chen, G. Hefter, and R. Buchner, J. Phys. Chem. A **107**, 4025 (2003).

[50] W. Wachter, W. Kunz, R. Buchner, and G. Hefter, J. Phys. Chem. A **109**, 8675 (2005).

[51] D. Huppert, V. Ittah, and E.M. Kosower, Chem Phys Lett **159**, 267 (1989).

[52] C.F. Chapman and M. Maroncelli, J Phys Chem **95**, 9095 (1991).

[53] V. Ittah and D. Huppert, Chem Phys Lett **173**, 496 (1990).

[54] E. Bart and D. Huppert, Chem Phys Lett **195**, 37 (1992).

[55] A. Chandra, J. Chem. Phys. **113**, 903 (2000).

[56] S. Chowdhuri and A. Chandra, J. Chem. Phys. **115**, 3732 (2001).

[57] J.M. Caillol, D. Levesque, and J.J. Weis, J Chem Phys **85**, 6645 (1986).

[58] G. Löffler, H. Schreiber, and O. Steinhauser, J Chem Phys **107**, 3135 (1997).

[59] A. Chandra, Phys. Rev. Lett. **85**, 768 (2000).

[60] A. Chandra, D. Wei, and G.N. Patey, J. Chem. Phys. **98**, 4959 (1993).

[61] A. Chandra and G.N. Patey, J. Chem. Phys. **100**, 8385 (1994).

[62] C. Schröder, T. Rudas, and O. Steinhauser, J. Chem. Phys. **125**, 244506 (2006).

[63] C. Schröder, T. Rudas, G. Neumayr, S. Benkner, and O. Steinhauser, J. Chem. Phys. **127**, 234503 (2007).

[64] C. Schröder and O. Steinhauser, J. Chem. Phys. **131**, 114504 (2009).

[65] C. Schröder and O. Steinhauser, J. Chem. Phys. **133**, 154511 (2010).

[66] C. Schröder, T. Sonnleitner, R. Buchner, and O. Steinhauser, Physical Chemistry Chemical Physics **13**, 12240 (2011).

[67] C. Schröder, M. Sega, M. Schmollngruber, E. Gailberger, D. Braun, and O. Steinhauser, J. Chem. Phys. **140**, 204505 (2014).

[68] C. Daguenet, P.J. Dyson, I. Krossing, A. Oleinikova, J. Slattery, C. Wakai, and H. Weingärtner, J Phys Chem B **110**, 12682 (2006).

[69] S. Schrödle, G. Annat, D.R. MacFarlane, M. Forsyth, R. Buchner, and G. Hefter, Chem. Commun. 1748 (2006).

[70] D.A. Turton, J. Hunger, A. Stoppa, G. Hefter, A. Thoman, M. Walther, R. Buchner, and K. Wynne, J Am Chem Soc **131**, 11140 (2009).

[71] E.W. Castner, C.J. Margulis, M. Maroncelli, and J.F. Wishart, Annu Rev Phys Chem **62**, 85 (2011).

[72] H. Jin, B. O'Hare, J. Dong, S. Arzhantsev, G.A. Baker, J.F. Wishart, A.J. Benesi, and M. Maroncelli, J Phys Chem B **112**, 81 (2008).

[73] J.A. Ingram, R.S. Moog, N. Ito, R. Biswas, and M. Maroncelli, J Phys Chem B **107**, 5926 (2003).

[74] A. Gupta, H.S. Dhattarwal, and H.K. Kashyap, J Chem Phys **154**, 184702 (2021).

[75] H.K. Kashyap, C.S. Santos, N.S. Murthy, J.J. Hettige, K. Kerr, S. Ramati, J. Gwon, M. Gohdo, S.I. Lall-Ramnarine, J.F. Wishart, C.J. Margulis, and E.W. Castner, J Phys Chem B **117**, 15328 (2013).

[76] S. Indra, R. Subramanian, and S. Daschakraborty, J Mol Liq **331**, 115608 (2021).

[77] S. Indra and S. Daschakraborty, Journal of Chemical Sciences **130**, 3 (2018).

[78] S. Daschakraborty and R. Biswas, J Chem Phys **140**, 014504 (2014).

[79] S. Daschakraborty, T. Pal, and R. Biswas, J Chem Phys **139**, 164503 (2013).

[80] M.J. Abraham, D. van der Spoel, E. Lindahl, B. Hess, and and the GROMACS development team, GROMACS User Manual version 2018, http://www.gromacs.org.

[81] W.L. Jorgensen, D.S. Maxwell, and J. Tirado-Rives, J. Am. Chem. Soc. **118**, 11225 (1996).

[82] J.A. Aguilar-Pineda, G.A. Méndez-Maldonado, E. Núñez-Rojas, and J. Alejandre, Mol. Phys. **113**, 2716 (2015).

[83] D.R. Lide and W.M. Haynes, editors, *CRC Handbook of Chemistry and Physics, 2009−2010, 90th Ed.*, 90th ed. (CRC Press, Boca Raton, FL, 2009).

[84] B. Doherty, X. Zhong, S. Gathiaka, B. Li, and O. Acevedo, J. Chem. Theory Comput. **13**, 6131 (2017).

[85] K.P. Jensen and W.L. Jorgensen, J. Chem. Theory Comput. **2**, 1499 (2006).

[86] L. Martinez, R. Andrade, E.G. Birgin, and J.M. Martínez, J. Comput. Chem. **30**, 2157 (2009).

[87] R.W. Hockney, S.P. Goel, J.W. Eastwood, R.W. Hockney, S.P. Goel, and J.W. Eastwood, JCoPh **14**, 148 (1974).

[88] B. Hess, H. Bekker, H.J.C. Berendsen, and J.G.E.M. Fraaije, J. Comput. Chem. **18**, 14631472 (1997).

[89] S. Nosé, Mol. Phys. **52**, 255 (1984).

[90] W.G. Hoover, Phys Rev A (Coll Park) **31**, 1695 (1985).

[91] M. Parrinello and A. Rahman, J. App. Phys. **52**, 7182 (1981).

[92] S. Nosé and M.L. Klein, Mol. Phys. **50**, 1055 (1983).

[93] G. Kalita, K.G. Sarma, and S. Mahiuddin, J. Chem. Eng. Data **44**, 222 (1999).

[94] L.C. Branco, Joa, O.N. Rosa, J.J.M. Ramos, and C.A.M. Afonso, (n.d.).

[95] W. Xu, E.I. Cooper, and C.A. Angell, Journal of Physical Chemistry B **107**, 6170 (2003).

[96] H. Tokuda, K. Hayamizu, K. Ishii, M.A.B.H. Susan, and M. Watanabe, J. Phys. Chem. B **108**, 16593 (2004).

[97] M.L.T. Asaki, A. Redondo, T.A. Zawodzinski, and A.J. Taylor, J. Chem. Phys. **116**, 10377 (2002).

[98] B. Bagchi and R. Biswas, in *Adv Chem Phys* (1999), pp. 207–433.

[99] S. Arzhantsev, H. Jin, G.A. Baker, and M. Maroncelli, J. Phys. Chem.. B **111**, 4978 (2007).

[100] X. Song, J. Chem. Phys. **131**, (2009).

[101] C. Daguenet, P.J. Dyson, I. Krossing, A. Oleinikova, J. Slattery, C. Wakai, and H. Weingärtner, J. Phys. Chem. B **110**, 12682 (2006).

[102] K.F. Rinne, S. Gekle, and R.R. Netz, J. Chem. Phys. **141**, 214502 (2014).

[103] J.P. Hansen and I.R. McDonald, *Theory of Simple Liquids*, 3rd ed. (Academic, 2006).

[104] M.D. Ediger, Annu. Rev. Phys. Chem. **51**, 99 (2000).

[105] S. Banerjee, P.Kr. Ghorai, S. Das, J. Rajbangshi, and R. Biswas, J. Chem. Phys. **153**, 234502 (2020).

[106] B.U. Felderhof, Mol. Phys. **51**, 801 (1984).

[107] F.E. Harris and C.T. O'Konski, J. Phys. Chem. **61**, 310 (1957).

[108] A.Yu. Zasetsky and I.M. Svishchev, J. Chem. Phys. **115**, 1448 (2001).

[109] J. Sala, E. Guàrdia, and J. Martí, J. Chem. Phys. **132**, 214505 (2010).

[110] S. Seal, K. Doblhoff-Dier, and J. Meyer, J. Phys. Chem. B **123**, 9912 (2019).

[111] P.E. Smith and W.F. van Gunsteren, J. Chem. Phys. **100**, 3169 (1994).

[112] L. Saiz, E. Guàrdia, and J.-À. Padró, J. Chem. Phys. **113**, 2814 (2000).

[113] S. Das, R. Biswas, and B. Mukherjee, J Phys Chem B **119**, 274 (2015).

[114] C. Caleman, P.J. van Maaren, M. Hong, J.S. Hub, L.T. Costa, and D. van der Spoel, J. Chem. Theory Comput. **8**, 61 (2012).

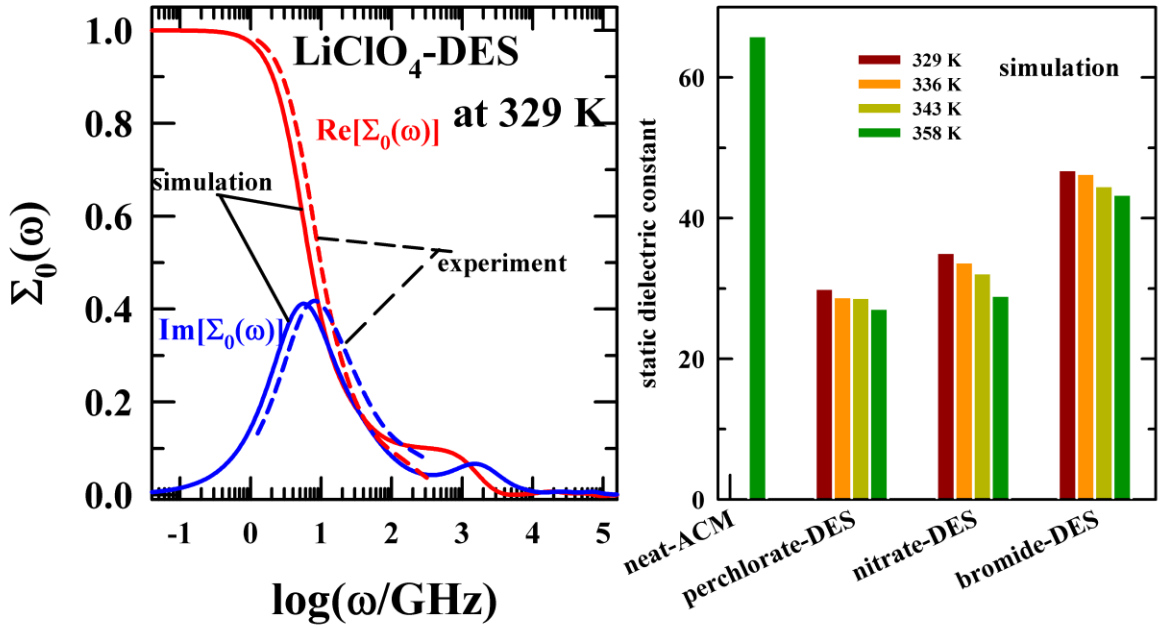

FIG. Graphical abstract